LETTER

doi:10.1038/nature13710

A 400-solar-mass black hole in the galaxy M82

Dheeraj R. Pasham[1,2], Tod E. Strohmayer[2] & Richard F. Mushotzky[1]

M82 X-1, the brightest X-ray source in the galaxy M82, has been thought to be an intermediate-mass black hole (100 to 10,000 solar masses) because of its extremely high luminosity and variability characteristics[1–6], although some models suggest that its mass may be only about 20 solar masses[3,7]. The previous mass estimates were based on scaling relations that use low-frequency characteristic timescales which have large intrinsic uncertainties[8,9]. For stellar-mass black holes, we know that the high-frequency quasi-periodic oscillations (100–450 hertz) in the X-ray emission that occur in a 3:2 frequency ratio are stable and scale in frequency inversely with black hole mass with a reasonably small dispersion[10–15]. The discovery of such stable oscillations thus potentially offers an alternative and less ambiguous means of mass determination for intermediate-mass black holes, but has hitherto not been realized. Here we report stable, twin-peak (3:2 frequency ratio) X-ray quasi-periodic oscillations from M82 X-1 at frequencies of 3.32 ± 0.06 hertz and 5.07 ± 0.06 hertz. Assuming that we can extrapolate the inverse-mass scaling that holds for stellar-mass black holes, we estimate the black hole mass of M82 X-1 to be 428 ± 105 solar masses. In addition, we can estimate the mass using the relativistic precession model, from which we get a value of 415 ± 63 solar masses.

Oscillations arising from general relativistic effects should scale inversely with black hole mass if they arise from orbital motion near the innermost stable circular orbit in the accretion disk[16,17], and there is observational support that they do for stellar-mass black holes[10] (3–50 solar masses ($M_{\odot}$)). Previous estimates of the mass of M82 X-1, of a few

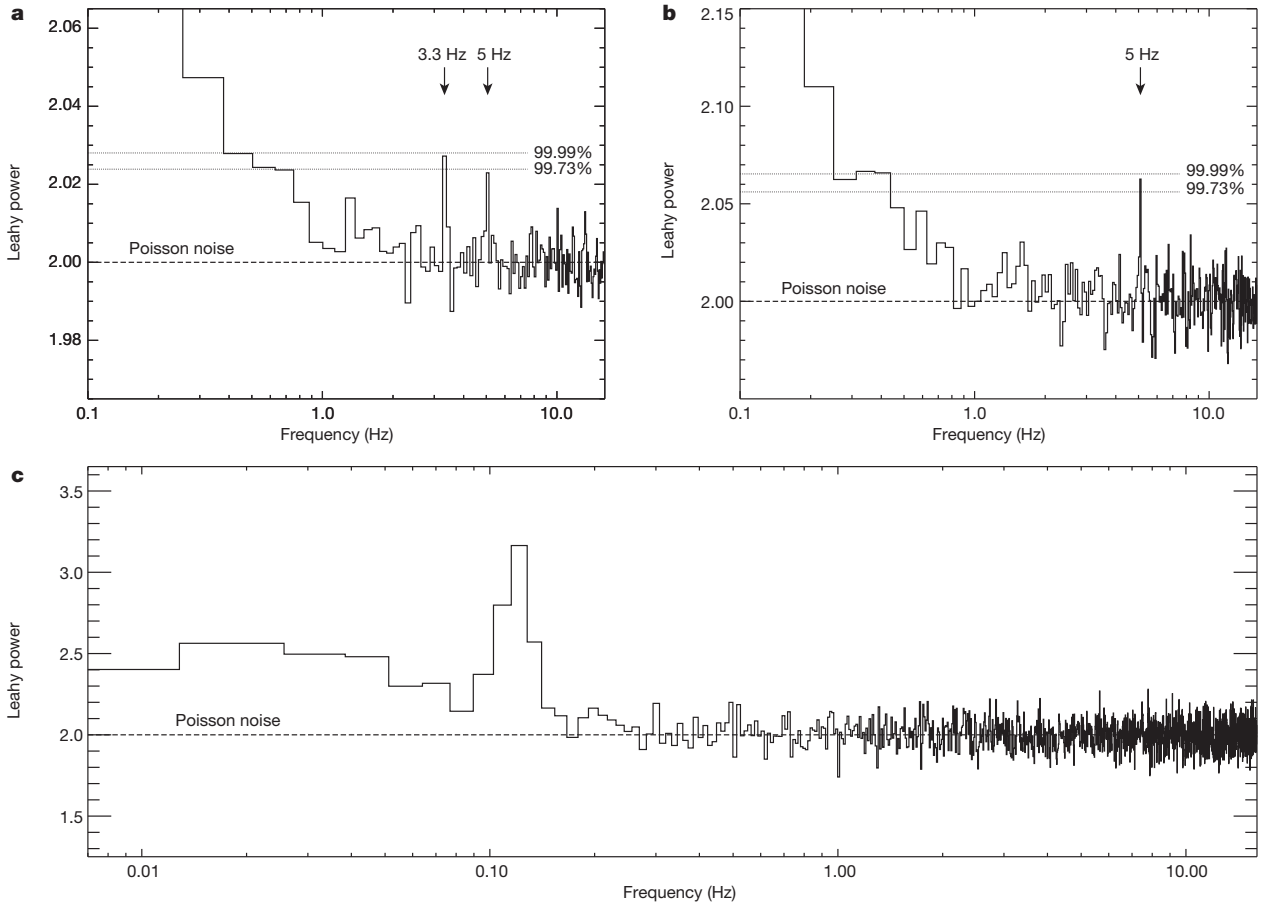

Figure 1 | Power density spectra of M82. **a**, Six-year average X-ray (3–13 keV) power density spectrum of M82 using 7,362 individual 128 s light curves. The frequency resolution is 0.125 Hz. The two strongest features in the power spectrum occur at 3.32 ± 0.06 and 5.07 ± 0.06 Hz, consistent with a 3:2 frequency ratio. **b**, Averaged power density spectrum of all (363) 1,024 s segments. The frequency resolution is 0.0625 Hz. The strongest feature is at 5 Hz. **c**, For a direct comparison with stellar-mass black holes, we show the broadband power density spectrum of M82 (using ~100 ks of XMM-Newton/EPIC data; ID: 0206080101) showing the low-frequency quasi-periodic oscillation at 120 mHz in addition to the high-frequency quasi-periodic oscillation pair in **a** and **b**. Power spectra are Leahy-normalized to a value of 2.

[1]Astronomy Department, University of Maryland, College Park, Maryland 20742, USA. [2]Astrophysics Science Division and Joint Space-Science Institute, NASA Goddard Space Flight Center, Greenbelt, Maryland 20771, USA.

hundred solar masses, combined with the type-C identification[2,4,9] of its millihertz X-ray quasi-periodic oscillations, suggest that 3:2-ratio, twin-peak, high-frequency oscillations analogous to those seen in stellar-mass black holes, if present, should be detectable in the frequency range of a few hertz[16]. We accordingly searched NASA's Rossi X-ray Timing Explorer proportional counter array (PCA) archival data to look for 3:2 ratio oscillation pairs in the frequency range of 1–16 Hz, which corresponds to a black hole mass range of $50M_{\odot}$–$2{,}000M_{\odot}$.

We detected two power spectral peaks at 3.32 ± 0.06 Hz (with a coherence, the ratio of frequency to width, of $Q = \nu/\Delta\nu > 27$) and 5.07 ± 0.06 Hz ($Q > 40$), consistent with a 3:2 frequency ratio (Fig. 1a, b). The combined statistical significance of the detection is greater than 4.7σ (Methods).

The PCA's field of view ($1^{\circ} \times 1^{\circ}$) of M82 includes a number of accreting X-ray sources in addition to M82 X-1[18]. The remarkable stability of the two quasi-periodic oscillations on timescales of a few years (Supplementary Videos 1 and 2), their 3:2 frequency ratio and their high oscillation luminosities strongly suggest they are not low-frequency quasi-periodic oscillations from a contaminating stellar-mass black hole (Methods). Also, a pulsar origin is very unlikely for several reasons. First, a pulsar signal would be much more coherent than that of the observed quasi-periodic oscillations, which have a finite width. Second, judging from the observed high quasi-periodic oscillation luminosities, it is extremely implausible that they originate from a pulsar (Methods). Finally, it would be highly unlikely to have two pulsars in the same field of view with spins in the 3:2 ratio. Also, on the basis of the average power spectrum of the background sky and a sample of accreting supermassive black holes monitored by the PCA in the same epoch as M82, we rule out an instrumental origin for these oscillations (Extended Data Figs 2–4). This leaves M82 X-1, which is persistently the brightest source in the field of view, as the most likely source associated with the 3:2-ratio quasi-periodic oscillation pair.

We estimated M82 X-1's black hole mass, assuming first the inverse-mass scaling of stellar-mass black holes and then the relativistic precession model[19,20], to be $(428 \pm 105)M_{\odot}$ in the first case and $(415 \pm 63)M_{\odot}$ in the second (Fig. 2). Combining the average 2–10 keV X-ray luminosity[21,22] of the source, of 5×10^{40} erg s^{-1}, with the measured mass suggests that the source is accreting close to the Eddington limit with an accretion efficiency of 0.8 ± 0.2.

The previous mass measurements of M82 X-1 have large uncertainties owing to both systematic and measurement errors. For example, modelling of its X-ray energy spectra during the thermal-dominant state using a fully relativistic, 'multicoloured' disk model suggests that it hosts an intermediate-mass black hole that has a mass anywhere in the range of $200M_{\odot}$–$800M_{\odot}$ and is accreting near the Eddington limit[3]. In addition to the large mass uncertainty associated with the modelling, the same study also found that the energy spectra can be equally well fit with a stellar-mass black hole accreting at a rate ~160 higher than the Eddington limit[3]. Also, the X-rays from this source are known to modulate with a periodicity of 62 days, which has been argued to be the orbital period of an intermediate-mass black hole[22]—formed in the nearby star cluster MCG-11 by stellar runaway collisions[5,23,24]—accreting matter via Roche lobe overflow from a $22M_{\odot}$–$25M_{\odot}$ companion star[24]. Detailed stellar binary evolution simulations suggest that the long periodicity is best explained by an intermediate-mass black hole with mass in the range of $200M_{\odot}$–$5{,}000M_{\odot}$ (refs 5, 24). However, a recent study finds that this periodicity may instead be due to a precessing accretion disk, in which case a stellar-mass black hole will suffice to explain the apparent long periodicity[21].

One of the main lines of argument for an intermediate-mass black hole in M82 X-1 follows from the assumption that its millihertz quasi-periodic oscillations are analogous to the type-C oscillations of stellar-mass black holes and to scale the inverse-mass relationship of the frequency of these millihertz oscillations (frequency range of 37–210 mHz (refs 9, 25); Fig. 1c) to the type-C, low-frequency X-ray oscillations (frequency range of 0.2–15 Hz (refs 10, 26)). There are two uncertainties with such scaling: first, it was unclear—until now—whether these millihertz oscillations are indeed the type-C analogues of stellar-mass black holes[8,9], and, second, both the type-C and the millihertz oscillations are variable, resulting in a large dispersion in the measured mass of $25M_{\odot}$–$1{,}300M_{\odot}$ (refs 1, 2, 4, 6). The simultaneous discovery of stable, 3:2 ratio, high-frequency periodicities and low-frequency millihertz oscillations allows us to set the overall frequency scale of the X-ray power spectrum. This result not only implies that the millihertz quasi-periodic oscillations of M82 X-1 are the type-C analogues of stellar-mass black holes, but also provides an independent, and so far the most accurate, black hole mass measurement.

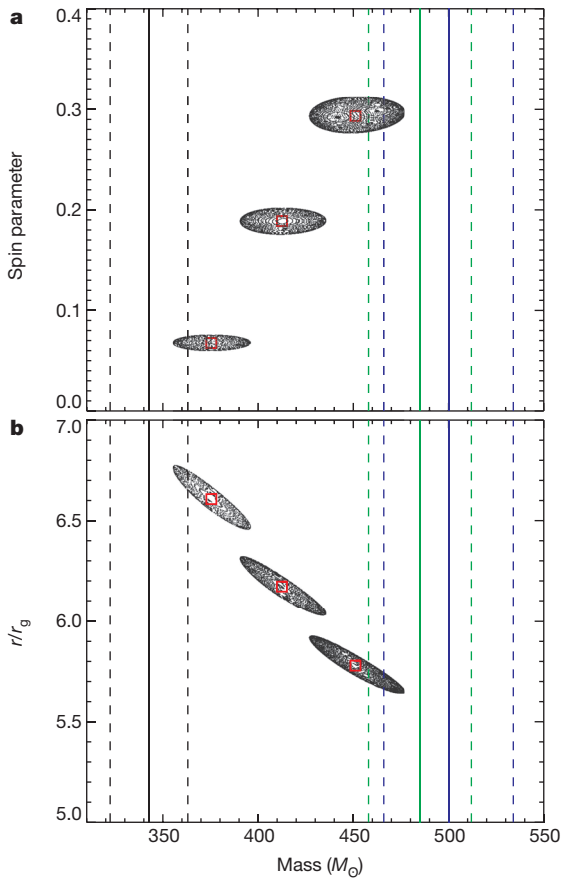

Figure 2 | Mass, spin and radius measurements. **a**, Contours (90% confidence) of M82 X-1's mass as a function of the spin parameter, that is, the ratio of the black hole's angular momentum to its mass. The three contours correspond to the three low frequency values (37, 120 and 210 mHz), with the mass increasing as the low-frequency oscillation frequency increases. **b**, Contours of M82 X-1's mass as a function of the radius of the origin of these oscillations (in units of $r_g = GM/c^2$, where G, M and c are the gravitational constant, the black hole mass and the speed of light, respectively). In **a** and **b**, the vertical lines (solid, solution; dashed, upper and lower limits) represent M82 X-1's mass estimates assuming a simple inverse-mass scaling for the high-frequency quasi-periodic oscillations. The three colours correspond to scalings using the microquasars GRO J1655-40[28] (green), XTE J1550-64[29] (blue) and GRS 1915+105[30] (black).

Finally, it should be pointed out that although the root mean squared amplitudes (3–5% of the X-ray flux) of the oscillations reported here, and their frequencies with respect to the millihertz oscillations (a few orders of magnitude higher), are similar to those observed in stellar-mass black holes[10], they appear narrower (with Q values of 27, 40 and 80) than stellar-mass black holes, which have Q values of <20 (refs 14, 27). In stellar-mass black holes, the Q factor seems to be energy dependent in some cases[14], and it is plausible that a similar effect may be operating in this case.

Online Content Methods, along with any additional Extended Data display items and Source Data, are available in the online version of the paper; references unique to these sections appear only in the online paper.

Received 25 April; accepted 21 July 2014.
Published online 17 August 2014.

1. Casella, P. *et al.* Weighing the black holes in ultraluminous X-ray sources through timing. *Mon. Not. R. Astron. Soc.* **387,** 1707–1711 (2008).
2. Dewangan, G. C., Titarchuk, L. & Griffiths, R. E. Black hole mass of the ultraluminous X-ray source M82 X-1. *Astrophys. J.* **637,** L21–L24 (2006).
3. Feng, H. & Kaaret, P. Identification of the X-ray thermal dominant state in an ultraluminous X-ray source in M82. *Astrophys. J.* **712,** L169–L173 (2010).
4. Mucciarelli, P., Casella, P., Belloni, T., Zampieri, L. & Ranalli, P. A variable quasi-periodic oscillation in M82 X-1. Timing and spectral analysis of XMM-Newton and RossiXTE observations. *Mon. Not. R. Astron. Soc.* **365,** 1123–1130 (2006).
5. Patruno, A., Portegies Zwart, S., Dewi, J. & Hopman, C. The ultraluminous X-ray source in M82: an intermediate-mass black hole with a giant companion. *Mon. Not. R. Astron. Soc.* **370,** L6–L9 (2006).
6. Zhou, X.-L., Zhang, S.-N., Wang, D.-X. & Zhu, L. Calibrating the correlation between black hole mass and X-ray variability amplitude: X-ray only black hole mass estimates for active galactic nuclei and ultra-luminous X-ray sources. *Astrophys. J.* **710,** 16–23 (2010).
7. Okajima, T., Ebisawa, K. & Kawaguchi, T. A stellar-mass black hole in the ultraluminous X-ray source M82 X-1? *Astrophys. J.* **652,** L105–L108 (2006).
8. Middleton, M. J., Roberts, T. P., Done, C. & Jackson, F. E. Challenging times: a re-analysis of NGC 5408 X-1. *Mon. Not. R. Astron. Soc.* **411,** 644–652 (2011).
9. Pasham, D. R. & Strohmayer, T. E. On the nature of the mHz X-ray quasi-periodic oscillations from ultraluminous X-ray source M82 X-1: Search for timing-spectral correlations. *Astrophys. J.* **771,** 101 (2013).
10. McClintock, J. E. & Remillard, R. A. in *Compact Stellar X-Ray Sources* (eds Lewin, W. & van der Klis, M.) 157–213 (Cambridge Univ. Press, 2006).
11. Remillard, R. A., Morgan, E. H., McClintock, J. E., Bailyn, C. D. & Orosz, J. A. RXTE observations of 0.1–300 HZ quasi-periodic oscillations in the microquasar GRO J1655–40. *Astrophys. J.* **522,** 397–412 (1999).
12. Remillard, R. A., Muno, M. P., McClintock, J. E. & Orosz, J. A. Evidence for harmonic relationships in the high-frequency quasi-periodic oscillations of XTE J1550–564 and GRO J1655–40. *Astrophys. J.* **580,** 1030–1042 (2002).
13. Remillard, R. A., Sobczak, G. J., Muno, M. P. & McClintock, J. E. Characterizing the quasi-periodic oscillation behavior of the X-ray nova XTE J1550–564. *Astrophys. J.* **564,** 962–973 (2002).
14. Strohmayer, T. E. Discovery of a 450 HZ quasi-periodic oscillation from the microquasar GRO J1655–40 with the Rossi X-Ray Timing Explorer. *Astrophys. J.* **552,** L49–L53 (2001).
15. Strohmayer, T. E. Discovery of a second high-frequency quasi-periodic oscillation from the microquasar GRS 1915+105. *Astrophys. J.* **554,** L169–L172 (2001).
16. Abramowicz, M. A., Kluźniak, W., McClintock, J. E. & Remillard, R. A. The importance of discovering a 3:2 twin-peak quasi-periodic oscillation in an ultraluminous X-ray source, or how to solve the puzzle of intermediate-mass black holes. *Astrophys. J.* **609,** L63–L65 (2004).
17. Abramowicz, M. A. & Kluźniak, W. Interpreting black hole QPOs. Preprint at http://arxiv.org/abs/astro-ph/0312396 (2003).
18. Matsumoto, H. *et al.* Discovery of a luminous, variable, off-center source in the nucleus of M82 with the Chandra High-Resolution Camera. *Astrophys. J.* **547,** L25–L28 (2001).
19. Stella, L., Vietri, M. & Morsink, S. M. Correlations in the quasi-periodic oscillation frequencies of low-mass X-ray binaries and the relativistic precession model. *Astrophys. J.* **524,** L63–L66 (1999).
20. Motta, S. E., Belloni, T. M., Stella, L., Munoz-Darias, T. & Fender, R. Precise mass and spin measurements for a stellar-mass black hole through X-ray timing: the case of GRO J1655–40. *Mon. Not. R. Astron. Soc.* **437,** 2554–2565 (2014).
21. Pasham, D. R. & Strohmayer, T. E. Can the 62 day X-ray period of ULX M82 X-1 be due to a precessing accretion disk? *Astrophys. J.* **774,** L16 (2013).
22. Kaaret, P. & Feng, H. Confirmation of the 62 day X-ray periodicity from M82. *Astrophys. J.* **669,** 106–108 (2007).
23. Voss, R., Nielsen, M. T. B., Nelemans, G., Fraser, M. & Smartt, S. J. On the association of ULXs with young superclusters: M82 X-1 and a new candidate in NGC 7479. *Mon. Not. R. Astron. Soc.* **418,** L124 (2011).
24. Portegies Zwart, S. F., Baumgardt, H., Hut, P., Makino, J. & McMillan, S. L. W. Formation of massive black holes through runaway collisions in dense young star clusters. *Nature* **428,** 724–726 (2004).
25. Caballero-García, M. D., Belloni, T. & Zampieri, L. Quasi-periodic oscillations and energy spectra from the two brightest ultra-luminous X-ray sources in M82. *Mon. Not. R. Astron. Soc.* **436,** 3262–3270 (2013).
26. Casella, P., Belloni, T. & Stella, L. The ABC of low-frequency quasi-periodic oscillations in black hole candidates: analogies with Z sources. *Astrophys. J.* **629,** 403–407 (2005).
27. Belloni, T. M., Sanna, A. & Mèndez, M. High-frequency quasi-periodic oscillations in black hole binaries. *Mon. Not. R. Astron. Soc.* **426,** 1701–1709 (2012).
28. Beer, M. E. & Podsiadlowski, P. The quiescent light curve and the evolutionary state of GRO J1655–40. *Mon. Not. R. Astron. Soc.* **331,** 351–360 (2002).
29. Orosz, J. A. *et al.* An improved dynamical model for the microquasar XTE J1550–564. *Astrophys. J.* **730,** 75–88 (2011).
30. Steeghs, D. *et al.* The not-so-massive black hole in the microquasar GRS1915+105. *Astrophys. J.* **768,** 185–192 (2013).

Supplementary Information is available in the online version of the paper.

Acknowledgements This work is based on observations made with the Rossi X-ray Timing Explorer, a mission that was managed and controlled by NASA's Goddard Space Flight Center in Greenbelt, Maryland, USA. All the data used in the present article is publicly available through NASA's HEASARC archive. D.R.P. would like to thank M. Trippe, C. Miller and C. Reynolds for discussions.

Author Contributions D.R.P. and T.E.S. reduced the data, carried out the analysis and wrote the paper. R.F.M. contributed to the interpretation of the results.

Author Information Reprints and permissions information is available at www.nature.com/reprints. The authors declare no competing financial interests. Readers are welcome to comment on the online version of the paper. Correspondence and requests for materials should be addressed to D.R.P. (dheeraj@astro.umd.edu).

METHODS

Estimating the expected significance of the quasi-periodic oscillations. The detectability (statistical significance, n_σ) of a quasi-periodic oscillation feature can be expressed as

$$n_\sigma = \frac{1}{2} r^2 \frac{S^2}{S+B} \sqrt{\frac{T}{\Delta\nu}}$$

where r, S, B, T and $\Delta\nu$ are the root mean squared (r.m.s.) amplitude of the quasi-periodic oscillation, the source count rate, the background count rate, the exposure time and the width of the quasi-periodic oscillation, respectively[31]. Assuming an r.m.s. amplitude of a few per cent—similar to that seen in stellar-mass black holes[27]—and using the mean Rossi X-ray Timing Explorer (RXTE)/PCA source and background rates obtained from prior observations[21], we found that the wealth of publicly available, archival RXTE monitoring data ($\sim 10^6$ s) spread across a time span of ~6 years would suffice for a sensitive search for high-frequency quasi-periodic oscillations in M82 X-1.

Data primer. M82 was monitored (0.5-2 ks roughly once every three days) with the RXTE/PCA between 1997 February 2 and 1997 November 25 (0.8 years) and between 2004 September 2 and 2009 December 30 (5.3 years). All the PCA observations were carried out in the GoodXenon data acquisition mode. The total number of monitoring observations was 867, which were divided among six proposals (RXTE proposal IDs P20303, P90121, P90171, P92098, P93123 and P94123). As recommended by the data analysis guide provided by the RXTE Guest Observer Facility (https://heasarc.gsfc.nasa.gov/docs/xte/abc/screening.html), we first screened the data to include only time intervals that satisfy the following criteria: ELV >10.0 && OFFSET <0.02 && (TIME SINCE SAA <0 || TIME SINCE SAA >30) && ELECTRON2 <0.1. In addition to the above standard filters, we used only X-ray events within the energy range of 3–13 keV, which translates to PCA channels 7–32. This energy range is comparable to the bandpass in which high-frequency quasi-periodic oscillations have been reported from stellar-mass black holes[10,14,15]. Moreover, beyond 13 keV the background dominates the overall count rate by a factor greater than 10. For each observation, we used all active proportional counter units, to maximize the count rate and, thus, the sensitivity to quasi-periodic oscillations.

Before we extracted the individual power spectra, we created individual light curves (using a bin size of 1 s) from all the observations. Through manual inspection we removed a small number of observations affected by flares, because these are attributed to background events, for example gamma-ray bursts, not associated with the source. Extended Data Fig. 1 shows two sample light curves and their corresponding power spectra. They represent the typical quality of the individual light curves used in extracting the average power spectra.

Estimating the statistical significances. We first divided the data into 128 s segments and extracted their light curves with a time resolution of 1/32 s. We then constructed a Leahy-normalized[32] power density spectrum (where the Poisson noise level is 2) from each of these 128 s light curves. All the power spectra were then combined (7,362 individual power spectra) to obtain a six-year-averaged power density spectrum of M82 (Fig. 1a).

To estimate the statistical significance of any features in the 1–16 Hz range of the six-year-averaged power density spectrum obtained using the 128 s data segments, we first ensured that the local mean was equal to 2, the value expected from a purely Poisson (white noise) process. We then computed the probability, at the 99.73% (3σ) and the 99.99% (3.9σ) confidence levels, of obtaining the power, $P = P_* \times 7{,}362 \times 16$ from a χ^2 distribution with $2 \times 7{,}362 \times 16$ degrees of freedom. Here P_* is the power value of a statistical fluctuation at a given confidence level. We used this χ^2 distribution because we summed 16 neighbouring frequency bins and divided by 16, and averaged 7,362 individual power spectra. Considering the total number of trials (frequency bins within 1–16 Hz), we computed the 99.73% (1/(371 trials)) and the 99.99% (1/(10,000 trials)) confidence limits (horizontal dotted lines in Fig. 1a). We detect two power spectral peaks at 3.32 ± 0.06 and 5.07 ± 0.06 Hz that are significant at the 2×10^{-4} (3.7σ) and 6×10^{-3} (2.75σ) levels, respectively, assuming both features were searched for independently between 1 and 16 Hz. However, after identifying the first feature at 3.3 Hz, if we are searching for a second feature at a 3:2 ratio, then the search from there on only includes the bins close to $3/2 \times 3.3$ Hz or $2/3 \times 3.3$ Hz. If this is taken into consideration, the significance of the 5 Hz feature increases, owing to the smaller number of trials, to 5×10^{-4}, or 3.5σ. To further test the significance of the 5 Hz feature, we extracted an average power density spectrum using all the data with segments longer than 1,024 s (Fig. 1b). The 5 Hz feature ($Q > 80$) is clearly detected at the 1.5×10^{-4} confidence level, or 3.8σ, considering a full search between 1 and 16 Hz.

The combined probability of two independent chance fluctuations in the 3:2 frequency ratio, one at the 3.7σ level (3.3 Hz feature) and the other at the 2.75σ level (5 Hz feature), is greater than 4.7σ.

Signal cannot be from a single observation. The very presence of these two features in the six-year-averaged power spectrum suggests that they are stable on this timescale. To further rule out the possibility that these oscillations are due to a single particular observation, or a small number of them, we constructed two dynamic average power spectra, one for the 128 s segments (dynamic power density spectrum#1; Supplementary Video 1) and another for the 1,024 s segments (dynamic power density spectrum#2; Supplementary Video 2). These track the evolution of the average power density spectra as a function of the total number of individual power spectra used in constructing the average. The two dynamic power density spectra clearly suggest that the power in these two features builds up gradually as more data are averaged, as opposed to appearing suddenly, which would be expected if a single or a small number of observations were contributing all the signal power. In addition, dynamic power density spectrum#1 clearly shows that while the 5 Hz feature is stronger during the earlier stages of the monitoring program, the 3.3 Hz feature is stronger during the later observations. Longer exposures of the order of 1–2 ks were carried out during the earlier stage of the monitoring program, which explains the higher significance of the 5 Hz feature in the average power density spectrum of the 1,024 s segments (Fig. 1b).

Root mean squared amplitude of the quasi-periodic oscillations. To calculate the r.m.s. variability amplitude of these quasi-periodic oscillations, we first determined the mean net count rate (source + background) of all the light curves used to extract the average power spectra. These values were equal to 29.9 counts s^{-1} and 35.2 counts s^{-1} for the power spectra with 128 s and 1,024 s segments, respectively. The r.m.s. amplitudes of the 3.3 and 5 Hz quasi-periodic oscillations, not correcting for the background, were estimated to be $1.1 \pm 0.1\%$ and $1.0 \pm 0.1\%$, respectively. Similarly, the r.m.s. amplitude of the 5 Hz feature in the power density spectrum with 1,024 s segments was estimated to be $1.1 \pm 0.1\%$. We then estimated the mean background count rate from the Standard2 data using the latest PCA background model. The mean background rates during the 128 s and the 1,024 s segments were estimated to be 18.9 counts s^{-1} and 24.0 counts s^{-1}, respectively. After accounting for the X-ray background, we find that the r.m.s. amplitudes of the 3.3 and 5 Hz features—averaged over all of the data—are $3.0 \pm 0.4\%$ and $2.7 \pm 0.4\%$, respectively, and the amplitude of the 5 Hz feature within the 1,024 s power density spectrum was estimated to be $3.5 \pm 0.4\%$.

Furthermore, the source count rates estimated above (net minus background) represent the combined contribution from all the X-ray point sources within the PCA's $1^\circ \times 1^\circ$ field of view[18]. Thus, the quasi-periodic oscillation r.m.s. amplitudes are underestimated. A study using the high-resolution camera on board Chandra suggests that there are multiple point sources within the $1' \times 1'$ region around M82 X-1[18,33]. Tracking the long-term variability of these sources suggests that the maximum luminosity reached by any of these sources—except for source 5 (as defined by ref. 18)—is less than one-fifth of the average luminosity of M82 X-1[33]. Source 5 is a highly variable transient ULX with a 0.5–10 keV luminosity varying between 10^{37} and 10^{40} erg s^{-1} (see the middle-left panel of fig. 1 of ref. 33). The quasi-periodic oscillations reported here are most probably produced by M82 X-1, which has persistently been the brightest source of any in the immediate vicinity of M82 X-1 (see the following sections). Although a precise value of the r.m.s. amplitude cannot be evaluated using the present data, we estimate an absolute upper limit by calculating the inverse of the fraction of the count rate contribution from M82 X-1, assuming all the remaining contaminating sources are at their brightest ever detected. This scenario is highly unlikely but will serve as an absolute upper bound on the r.m.s. amplitudes of the quasi-periodic oscillations, assuming they are from M82 X-1. Using the values reported by ref. 33, the fraction is roughly 1.8. Thus, the true r.m.s. amplitudes of the 3.3 and 5.5 Hz quasi-periodic oscillations are estimated to be in the range of 3–5%.

Also, XMM-Newton's EPIC instruments—with an effective area of about one-fifth of RXTE's PCA, albeit with lower background—observed M82 at multiple epochs, with a total effective exposure of ~350 ks. These observations were taken in the full-frame data acquisition mode with a time resolution of 73.4 ms or a Nyquist frequency of 6.82 Hz. This value is close to the quasi-periodic oscillation frequencies of interest and causes some signal suppression[31]. Nevertheless, we extracted an average 3–10 keV power density spectrum with 128 s data segments using all the observations (2,718 individual power spectra). We do not detect any statistically significant features near 3.3 and 5 Hz; however, we estimate quasi-periodic oscillation upper limits (3σ confidence) of 5.2 and 6.2% r.m.s. (using equations 4.4 and 4.10 of ref. 29) at 3.3 and 5 Hz, respectively, which are roughly twice the r.m.s. values of the quasi-periodic oscillations detected in the PCA data.

Using the 128 s data segments from RXTE, we also studied the energy dependence of the r.m.s. amplitudes of the two oscillations (Extended Data Table 1). Although the error bars are large, there seems to be a modest decrease in the r.m.s. amplitudes of these oscillations at lower X-ray energies. XMM-Newton's EPIC instruments are more sensitive in the 3–8 keV band, which is comparable to PCA channels 7–18 (the first and the fourth rows of Extended Data Table 1).

Ruling out low-frequency quasi-periodic oscillations. Low-frequency quasi-periodic oscillations of stellar-mass black holes, such as the type-C quasi-periodic oscillations[26], have typical centroid frequencies of a few hertz with r.m.s. amplitudes[26] of 5–25%, but are known to vary in frequency by factors of 8–10 over timescales of days[34,35]. This would lead to very broad features in the kind of average power spectrum we have used. Moreover, among the plethora of low-frequency quasi-periodic oscillations at present known, there is no indication of them preferentially occurring with a 3:2 frequency ratio. Furthermore, the average luminosity of the quasi-periodic oscillations reported here is ~0.03 times the average luminosity of all the sources observed by the PCA in the 3–13 keV band[21,22], which is $\sim 0.03 \times 5 \times 10^{40}\,\mathrm{erg\,s^{-1}} = 1.5 \times 10^{39}\,\mathrm{erg\,s^{-1}}$. This is comparable to or more than the peak X-ray luminosities of the contaminating sources, except for source 5 (refs 33, 36). Therefore, if these features were simply low-frequency quasi-periodic oscillations produced by any of the contaminating sources—except for source 5—their X-ray flux would have to be modulated at almost 100%, which is not plausible for the typical amplitudes of low-frequency quasi-periodic oscillations.

Source 5, which is a ULX, could in principle be the origin of these 3:2 ratio quasi-periodic oscillations. However, 3–4 mHz quasi-periodic oscillations have been discovered from this source and have been identified as type-A/B quasi-periodic oscillations analogues of stellar-mass black holes[37]. Such a characterization for the millihertz quasi-periodic oscillations suggests that the ULX might host a black hole with a mass of $12{,}000M_{\odot}$–$43{,}000M_{\odot}$ (ref. 37). If that were the case, the expected frequency range of high-frequency quasi-periodic oscillation analogues for a few-$10{,}000M_{\odot}$ black hole would be a few 100s of millihertz, which is a factor of 10 lower than the quasi-periodic oscillations reported here, suggesting that the 3.3 and 5 Hz quasi-periodic oscillations are less likely to be the high-frequency quasi-periodic oscillation analogues of source 5.

Ruling out pulsar origin. Rotation-powered pulsars can be strongly excluded, because they simply cannot provide the required luminosity. A neutron star's rotational energy loss rate can be expressed in terms of its moment of inertia, I, spin period, P, and period derivative, $\dot{P}$, as

$$\dot{E}_{\mathrm{rot}} = \frac{2\pi I \dot{P}}{P^3}$$

No known pulsar has a spin-down luminosity comparable to the estimated quasi-periodic oscillation X-ray luminosity. For example, the energetic Crab pulsar has $\dot{E} \approx 2 \times 10^{38}\,\mathrm{erg\,s^{-1}}$, and only a fraction of a pulsar's spin-down power typically appears as X-ray radiation. This rules out rotation-powered pulsars. Because M82 is a starburst galaxy, it probably hosts a population of accreting X-ray pulsars. Such accretion-powered pulsar systems are typically limited by the Eddington limit, of $\sim 2 \times 10^{38}\,\mathrm{erg\,s^{-1}}$, for a canonical neutron star. Useful comparisons can be made with the population observed with the RXTE/PCA in the Small Magellanic Cloud[38]. The authors of ref. 38 presented pulsed luminosities for the Small Magellanic Cloud pulsar population, and none was larger than $\sim 3 \times 10^{38}\,\mathrm{erg\,s^{-1}}$. Again, this is much smaller than the inferred quasi-periodic oscillations luminosities. Moreover, such pulsars are variable, and their time-averaged luminosities would be reduced further by their outburst duty cycles. At present, the only pulsar that is known to reach luminosities of $\sim 10^{40}\,\mathrm{erg\,s^{-1}}$ for brief periods of time is GRO J1744-28–the 'bursting pulsar'[39–41]. This object has a 2.1 Hz spin frequency and was discovered during an outburst that spanned the first 3 months of 1996 (we note that at the time of writing the source was detected in outburst again, suggesting a duty cycle of about 18 years[42–47]). Its peak persistent luminosity (assuming a distance close to that of the Galactic centre) was $\sim 7 \times 10^{38}\,\mathrm{erg\,s^{-1}}$. With a pulsed amplitude of about 10%, this would still give a pulsed luminosity much less than the inferred luminosities of the quasi-periodic oscillations. The type-II—accretion driven—bursts from this source[48] could reach about $10^{40}\,\mathrm{erg\,s^{-1}}$, and with a 10% pulsed amplitude this could give an instantaneous luminosity close to that of the average quasi-periodic oscillation luminosities. However, the bursting intervals make up less than 1% of the total time, and this small duty cycle will thus reduce the average pulsed luminosity due to the bursts to a level substantially below that of the observed quasi-periodic oscillations. Thus, we conclude that the observed quasi-periodic oscillations cannot be associated with accreting pulsars in M82.

Ruling out instrumental origin. We also rule out the possibility that this signal is intrinsic to RXTE/PCA by extracting the average power density spectra of a sample of accreting supermassive black holes with PCA count rates comparable to M82. To be consistent, we used only monitoring data taken in the GoodXenon mode during the same epoch as M82. The long-term light curves of these sources in the same time range as M82 are shown in Extended Data Fig. 2. On the basis of the causality argument, active galactic nuclei with black hole masses greater than $10^6 M_{\odot}$ cannot have coherent oscillations at frequencies higher than ~0.1 Hz. The average power spectra obtained with PCA in the 3–13 keV bandpass are essentially flat and are consistent with being Poisson noise (Extended Data Fig. 3). In addition, we also extracted the average power spectrum of a blank sky field (background) monitored using the GoodXenon mode during the same epoch as M82. The corresponding average power spectrum is shown in Extended Data Fig. 4b and is again consistent with being featureless, as expected.

Relativistic precession model analysis. According to the relativistic precession model, the upper harmonic of the high-frequency quasi-periodic oscillation is associated with the Keplerian frequency at some inner radius, and the lower harmonic of the high-frequency quasi-periodic oscillation and the type-C quasi-periodic oscillation are associated with the periastron and nodal precession frequencies, respectively, at the same radius. Recently, this model was applied to GRO J1655-40[20], which exhibits both low-frequency and high-frequency quasi-periodic oscillations and has a very accurate mass measurement of $(5.4 \pm 0.3)M_{\odot}$ (ref. 28). They find that the black hole mass evaluated from the relativistic precession model analysis agrees nicely with its dynamical mass estimate. Given this promise of the relativistic precession model, we estimated the mass and spin of M82 X-1's black hole using this model, essentially following the methodology in ref. 20.

The relativistic precession model analysis requires that the three quasi-periodic oscillations, the two high-frequency quasi-periodic oscillations and a low-frequency quasi-periodic oscillation, be observed simultaneously. This is, however, not the case for M82 observations. Although the combined six-year RXTE/PCA data show the high-frequency quasi-periodic oscillation pair, individual XMM-Newton observations randomly dispersed over the same epoch as the RXTE monitoring have shown low-frequency quasi-periodic oscillations with frequencies in the range of 37–210 mHz (see table 2 of ref. 10 and ref. 23). Thus, we carried out the analysis for three separate quasi-periodic oscillation frequencies, the lowest and the highest values (37 and 210 mHz, respectively) and a mean quasi-periodic oscillation frequency (120 mHz).

The dimensionless spin parameter is constrained to the range $0.06 < a < 0.31$, and the inferred radius, r, in the disk is in the range $5.53 < r/r_{\mathrm{g}} < 6.82$ (Fig. 2).

31. van der Klis, M. in *Timing Neutron Stars: Proc. NATO Adv. Study Inst. Timing Neutron Stars* (eds Ogelman, H. & van den Heuvel, E. P. J.) 27 (Kluwer Academic/Plenum, 1989).
32. Leahy, D. A. *et al.* On searches for pulsed emission with application to four globular cluster X-ray sources - NGC 1851, 6441, 6624, and 6712. *Astrophys. J.* **266,** 160–170 (1983).
33. Chiang, Y.-K. & Kong, A. K. H. The long-term variability of the X-ray sources in M82. *Mon. Not. R. Astron. Soc.* **414,** 1329–1338 (2011).
34. Wood, K. S. *et al.* USA experiment and RXTE observations of a variable low-frequency quasi-periodic oscillation in XTE J1118+480. *Astrophys. J.* **544,** L45–L48 (2000).
35. Rodriguez, J., Corbel, S., Kalemci, E., Tomsick, J. A. & Tagger, M. An X-ray timing study of XTE J1550-564: evolution of the low-frequency quasi-periodic oscillations for the complete 2000 outburst. *Astrophys. J.* **612,** 1018–1025 (2004).
36. Jin, J., Feng, H. & Kaaret, P. Transition to the disk dominant state of a new ultraluminous X-ray source in M82. *Astrophys. J.* **716,** 181–186 (2010).
37. Feng, H., Rao, F. & Kaaret, P. Discovery of millihertz X-ray oscillations in a transient ultraluminous X-ray source in M82. *Astrophys. J.* **710,** L137–L141 (2010).
38. Laycock, S. *et al.* Long-term behavior of X-ray pulsars in the Small Magellanic Cloud. *Astrophys. J.* **161,** 96–117 (2005).
39. Giles, A. B. *et al.* The main characteristics of GRO J1744-28 observed by the proportional counter array experiment on the Rossi X-Ray Timing Explorer. *Astrophys. J.* **469,** L25 (1996).
40. Jahoda, K. *et al.* Peak luminosities of bursts from GRO J1744-28 measured with the RXTE PCA. *Nucl. Phys. B Proc. Suppl.* **69**, 210–215 (1999).
41. Sazonov, S. Y., Sunyaev, R. A. & Lund, N. Super-Eddington X-ray luminosity of the bursting pulsar GRO J1744-28: WATCH/Granat observations. *Astron. Lett.* **23,** 286–292 (1997).
42. Negoro, H. *et al.* MAXI/GSC and Swift/BAT detection of enhanced hard X-ray emission from the Galactic center region, renewed activity of GRO J1744-28? *Astron. Telegr.* **5790** (2014).
43. Finger, M. H., Jenke, P. A. & Wilson-Hodge, C. Fermi/GBM detection of 0.467s pulsation from GRO J1744-28. *Astron. Telegr.* **5810** (2014).
44. Kennea, J. A., Kouveliotou, C. & Younes, G. GRO J1744-28: Swift XRT confirmation of outburst. *Astron. Telegr.* **5845** (2014).
45. D'Ai, A. *et al.* GRO J1744-28 active as X-ray pulsar. *Astron. Telegr.* **5858** (2014).
46. Linares, M., Kennea, J., Krimm, H. & Kouveliotou, C. Swift detects bursting activity from GRO J1744-28. *Astron. Telegr.* **5883** (2014).
47. Pintore, F. *et al.* Detection of a spin derivative in GRO J1744-28 with Swift/XRT. *Astron. Telegr.* **5901** (2014).
48. Kommers, J. M. *et al.* Postburst quasi-periodic oscillations from GRO J1744-28 and from the rapid burster. *Astrophys. J.* **482,** L53 (1997).

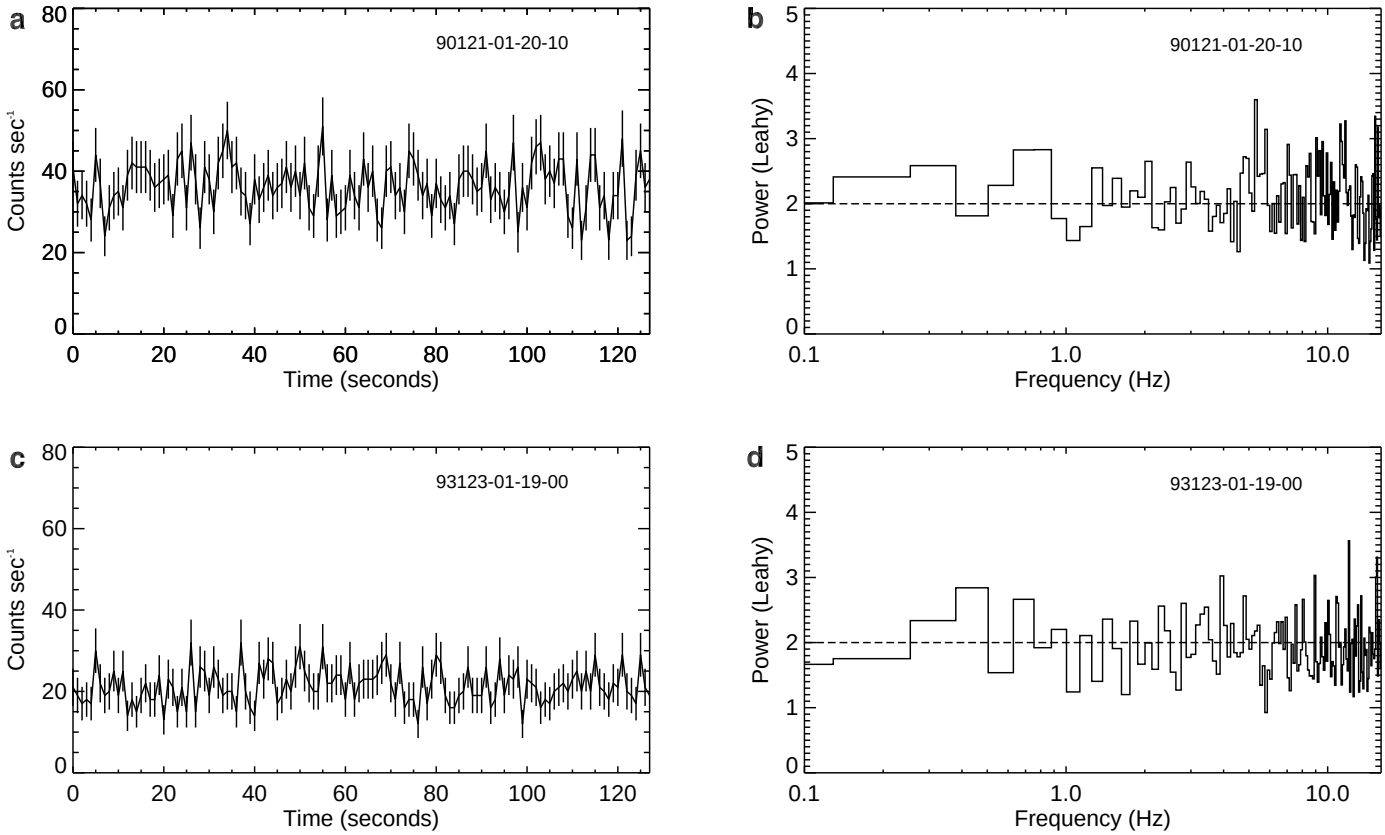

Extended Data Figure 1 | Sample RXTE/PCA light curves and power density spectra of M82. The 128 s X-ray (3–13 keV) light curves (**a**, **c**) and the corresponding power spectra (**b**, **d**) of M82. The corresponding observation IDs are shown in the top right of each panel. The light curves have a bin size of 1 s, and the power spectra have a frequency resolution of 0.125 Hz. The error bars in **a** and **c** represent the standard error of the mean.

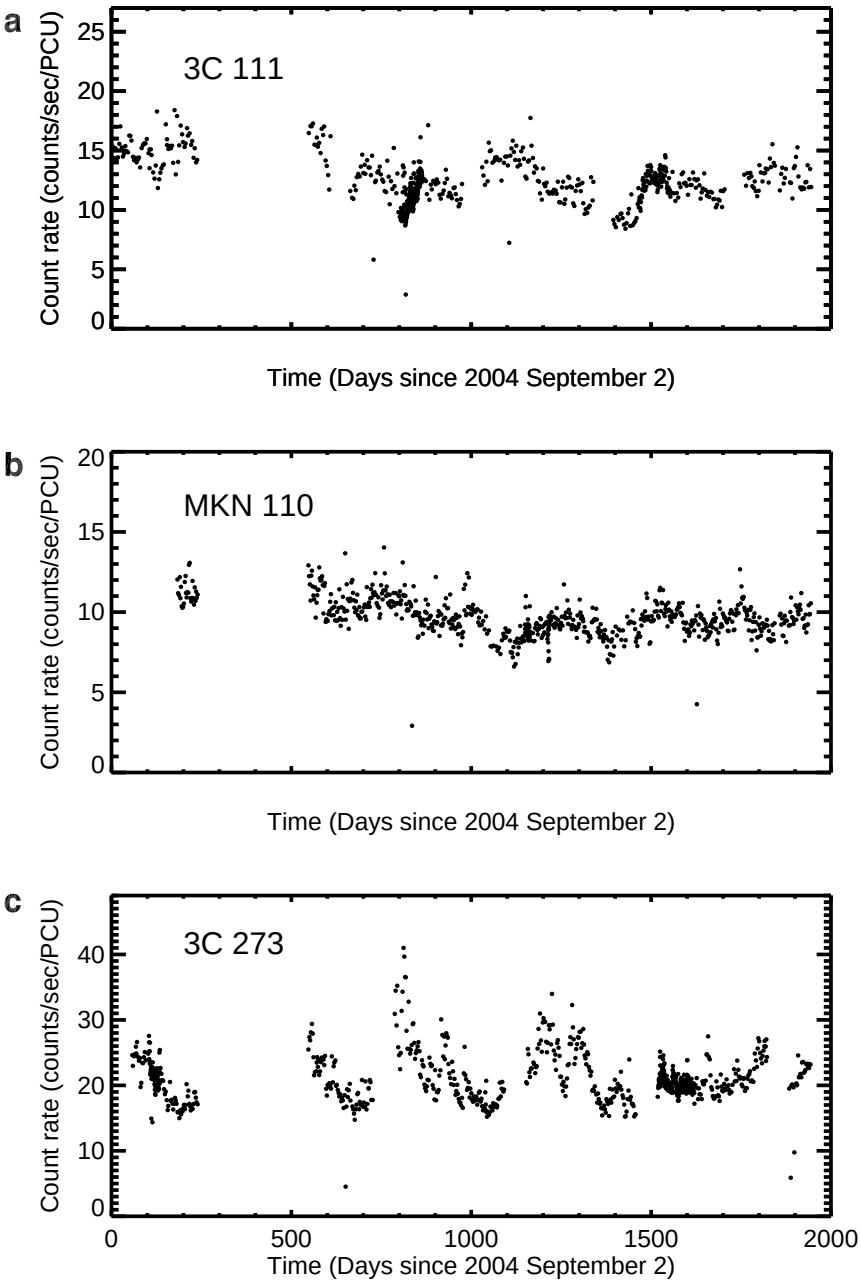

Extended Data Figure 2 | Long-term X-ray (3–13 keV) light curves of three accreting supermassive black holes. These were extracted from the same time window as the M82 observations (2004 September 2 to 2005 April 30 and 2006 March 3 to 2009 December 30). Data from 3C 111, MKN 110 and 3C 273 are shown in **a**, **b** and **c**, respectively. The count rates are not corrected for background.

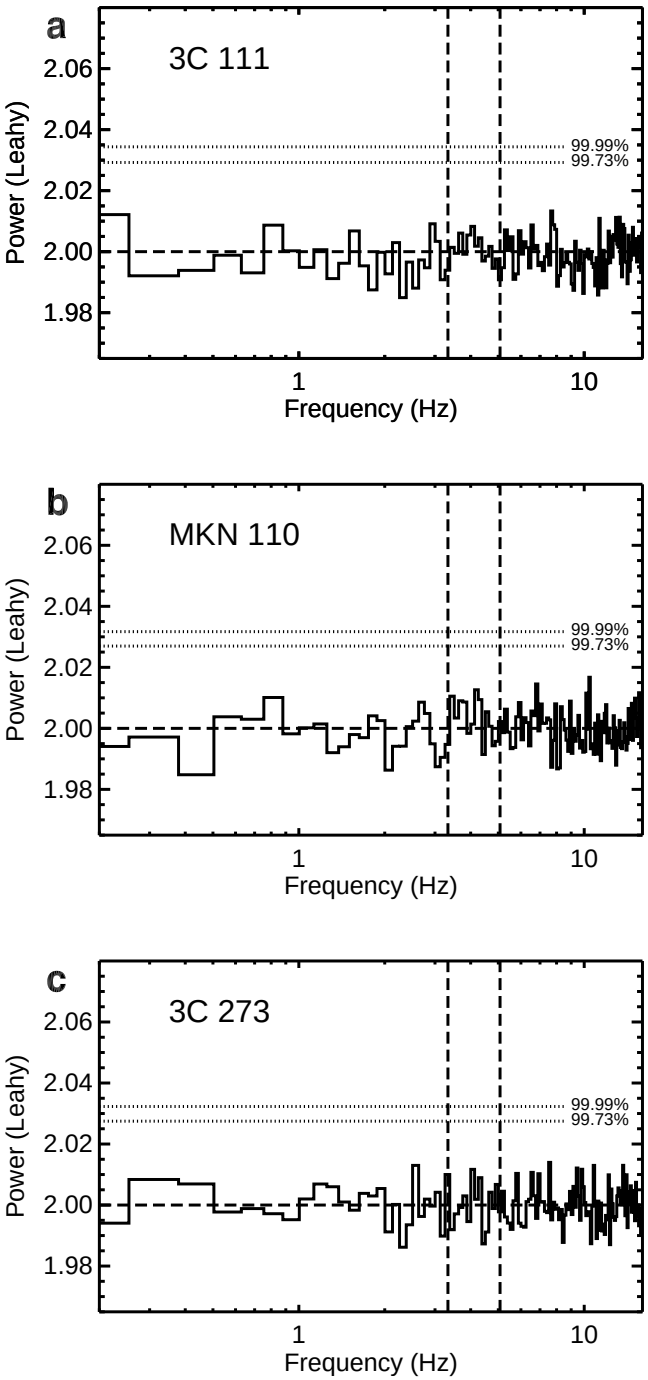

Extended Data Figure 3 | Average X-ray (3–13 keV) power spectra of three accreting supermassive black holes. Similar to the M82 analysis, these spectra were extracted by combining all the data (128 s data segments) shown in Extended Data Fig. 2. The Poisson noise level is equal to 2, and the 99.73% and 99.99% confidence contours are indicated by horizontal dotted lines. The two dashed vertical lines are drawn at 3.32 and 5.07 Hz. In all three cases, 3C 111 (**a**), MKN 110 (**b**) and 3C 273 (**c**), there are no significant power spectral features. The total PCA exposures used for these spectra were 630 ks (**a**), 738 ks (**b**) and 711 ks (**c**).

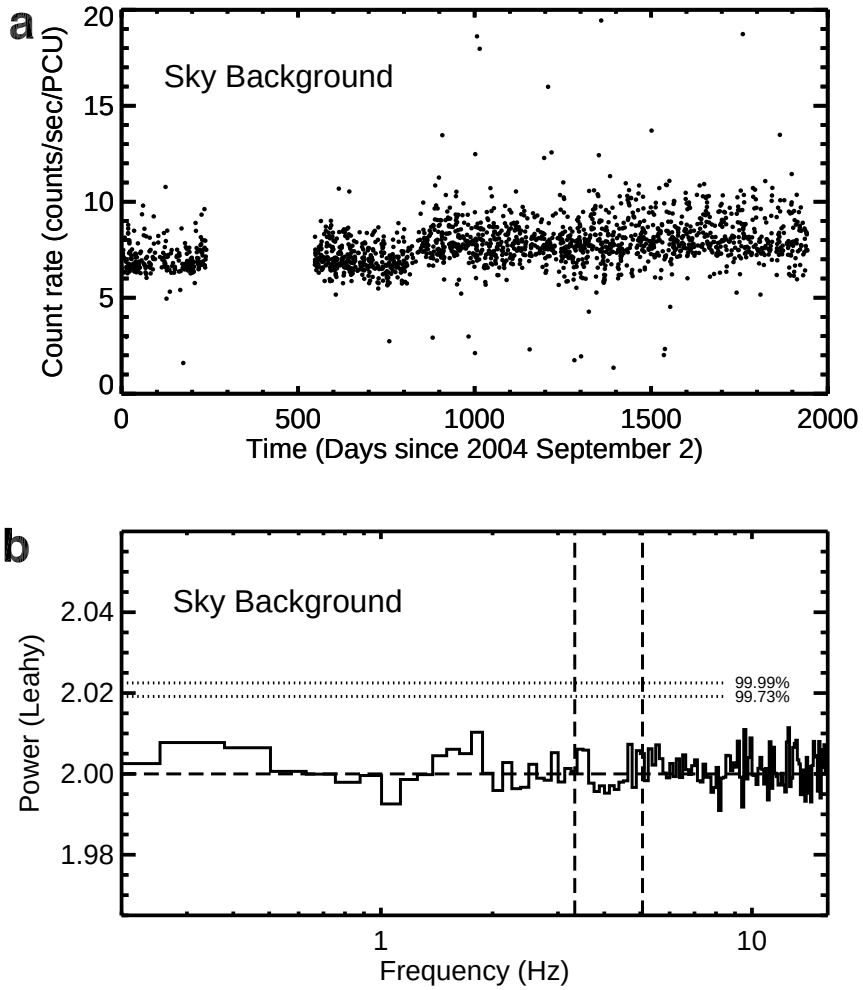

Extended Data Figure 4 | Long-term X-ray light curve and the average power density spectrum of a background sky field of RXTE/PCA. Similar to Extended Data Fig. 3, the 99.73% and 99.99% contours and the vertical lines at 3.32 and 5.07 Hz are indicated in the power density spectrum (**b**). Again, only observations coincident with M82 monitoring were used (2004 September 2 to 2005 April 30 and 2006 March 3 to 2009 December 30), and the total exposure time was 1,450 ks. The light curve (3–13 keV) is shown in (**a**). The background has coordinates of RA = 5.0°, dec. = −67.0°.

Extended Data Table 1 | Dependence of the percentage r.m.s. amplitudes of the two oscillations in the X-ray bandpass

PCA Channels	Energy Range	Net Count Rate[a]	Background Count Rate	Uncorrected % rms Amplitude[b]	Corrected % rms Amplitude[c]
3.32 Hz Quasi-Periodic Oscillation					
7-18	3-8 keV	19.0	10.5	1.1±0.2	2.8±0.4
7-24	3-10 keV	24.3	14.5	1.1±0.2	2.5±0.4
7-32	3-13 keV	29.9	18.9	1.1±0.1	2.7±0.4
5.07 Hz Quasi-Periodic Oscillation					
7-18	3-8 keV	19.0	10.5	1.2±0.2	2.5±0.4
7-24	3-10 keV	24.3	14.5	1.0±0.2	2.8±0.4
7-32	3-13 keV	29.9	18.9	1.0±0.1	3.0±0.4

* The total (source plus background) count rate in the given energy range (*a*).
† Not corrected for the background (*b*).
‡ Background-corrected percentage r.m.s. amplitude (*c*) where corrected r.m.s. amplitude = (uncorrected r.m.s. amplitude) × (total count rate)/(source count rate). The source count rate is the total rate minus the background rate. We used 128 s data segments for this study.